Measurement of the Permeability of a Cylinder of Grimsel Granite

A.P.S. Selvadurai
Department of Civil Engineering and Applied Mechanics
McGill University
817 Sherbrooke Street West
Montréal, QC, Canada H3A 0C3

Background

The primary objective of the exercise was to establish concensus in the measurement and interpretation of permeability of a typical rock in the low permeability range. The exact definition of where the high permeability stops and the low permeability starts is open to speculation since typical geomaterials tend to display a range of permeabilities: e.g. for sandstone: $\sim 10^{-15}$ m^2 to 10^{-12} m^2 (David et al,, 1994; Nabawy and David, 2016); for limestone:$\sim 10^{-15}$ m^2 to $\sim 10^{-14}$ m^2 (Selvadurai and Głowacki, 2008, Selvadurai and Selvadurai, 2010); concrete: $\sim 10^{-20}$ m^2 to $\sim 10^{-17}$ m^2 (Aldea et al., 1999; Mehta and Monteiro, 2014); cement grout: $\sim 10^{-21}$ m^2 to $\sim 10^{-20}$ m^2 (Selvadurai and Carnaffan, 1997); granite: $\sim 10^{-20}$ m^2 to $\sim 10^{-18}$ m^2 (Selvadurai *et al*., 2005; Selvadurai and Najari, 2013, 2015), Callovo-Oxfordian Argillite: $\sim 10^{-21}$ m^2 to $\sim 10^{-18}$ m^2 (Davy et al., 2007) and the Cobourg Limestone: $\sim 10^{-22}$ m^2 to $\sim 10^{-19}$ m^2 (Vilks and Miller, 2007; Selvadurai et al., 2011; Selvadurai and Jenner, 2012; Selvadurai and Głowacki, 2017). Thus, there is no strict definition of what constitutes a low permeability material; generally, rocks and other cementitious and synthetic materials with permeabilities less than 10^{-20} m^2 are regarded as low permeability materials. Measuring the permeability of such materials presents a challenge both from the experimental and modelling points of view.

There was considerable discussion about the selection of a material that was available in sufficient quantity and hydraulic uniformity that would enable the 29 participating research groups to conduct the very basic task of estimating the permeability of the candidate rock. After much deliberation and considering both synthetic and natural rocks, the leaders of the project chose to to use samples of the Grimsel Granite for the laboratory testing exercise. The ensuing report presents the test methodology and procedures utilized at the Environmental Geomechanics Laboratory at McGill University and summarizes the results of the tests.

The Sample

The characteristics of the Grimsel Granite sample were as follows (**Figures 1** and **2**):

Origin of Sample: Grimsel Test Site, Switzerland

Room Temperature: 23 ºC

Sample Diameter: D □□84.5 mm

Sample Height: H □□94 mm

Dry Mass of sample W = 1392.52 g

The Fluid Used

The fluid was normal non-degassed tap water with Viscosity

$\mu = 0.93 \times 10^{-6}$ kPa sec ; unit weight $\gamma_w = 9.81$ kN/m^3

Other Distinguishing Features: None

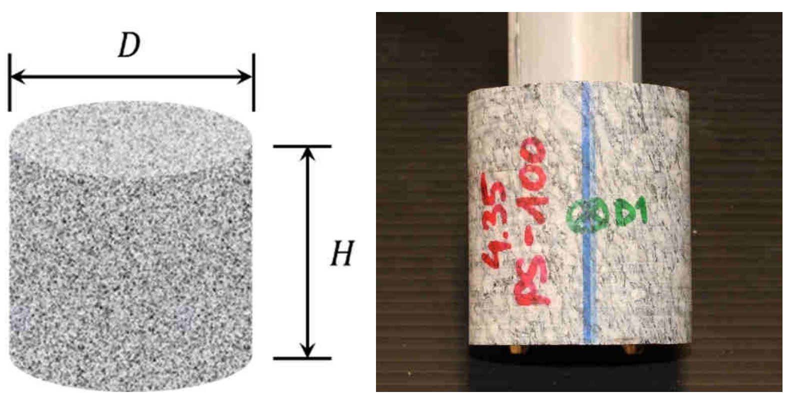

Figure 1. The cylindrical sample of Grimsel Granite

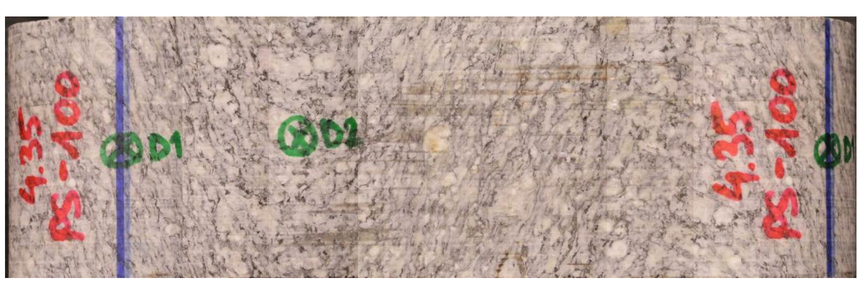

Figure 2. A panoramic view of the cylindrical surface

Testing Procedure

In view of the anticipated range of permeabilities, the permeability measurements were carried out using an Obert-Hoek cell where the axial and radial stresses could be applied independently. The schematic diagram of the Obert-Hoek Cell configuration, modified to accommodate the Grimsel Granite sample, is shown in Figure 3 and a general view of the experimental set up is shown in Figure 4. Details of the experimental components are shown in Figure 5.

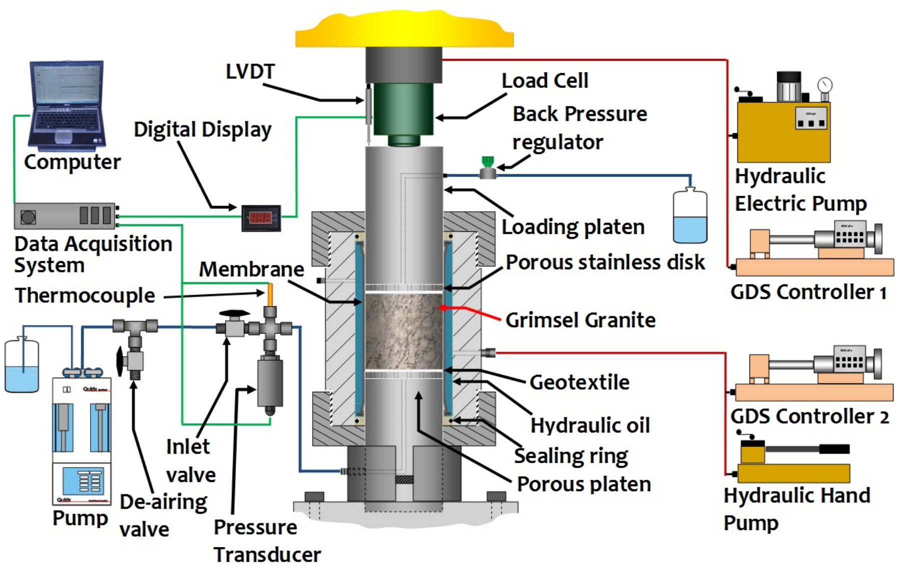

Figure 3. A schematic view of the McGill Obert-Hoek Cell facility

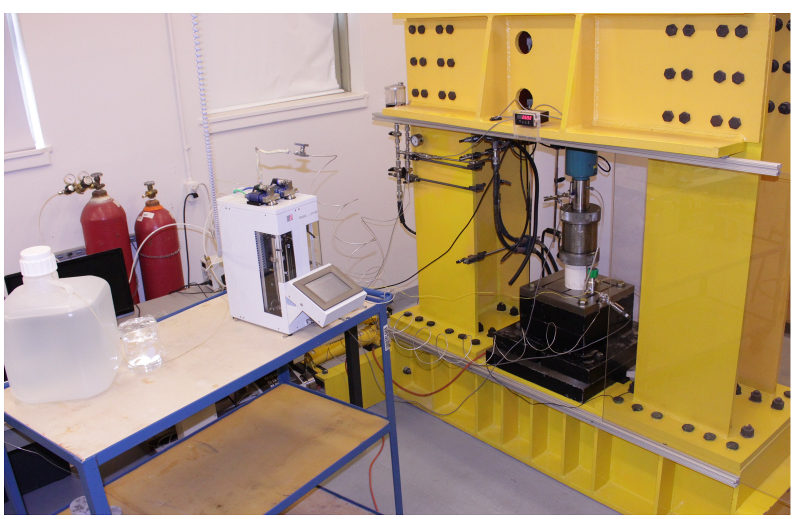

Figure 4. A general view of the laboratory arrangements

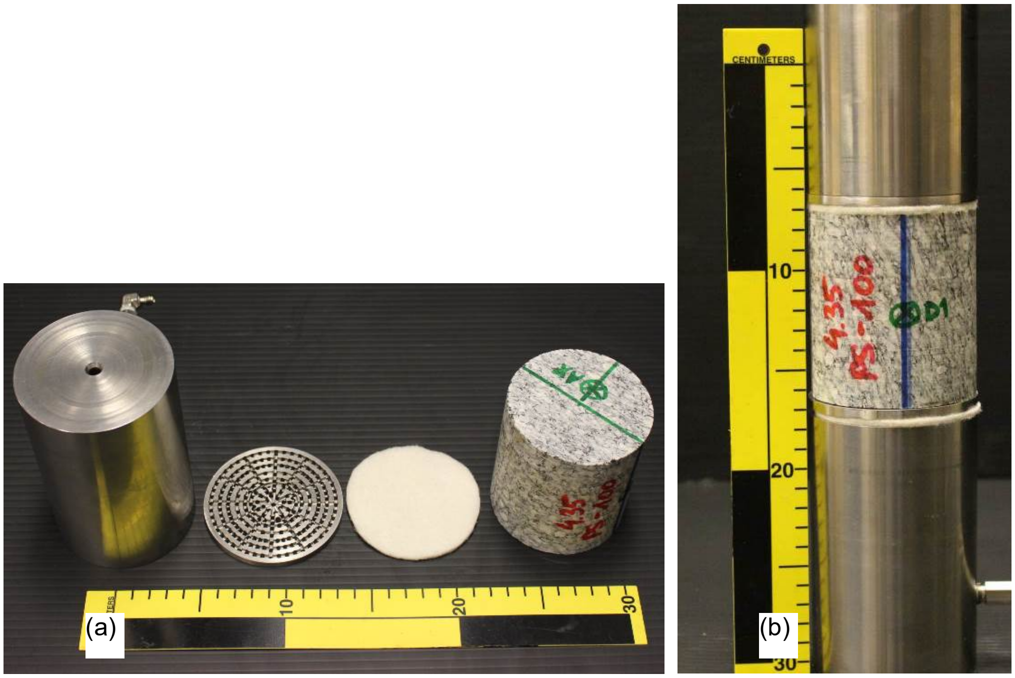

Figure 5: Components of the test set up. (a) from left to right: loading platen with central cavity for water flow, porous stainless steel disk for water distribution /collection, geotextile for friction reduction and water distribution and the Grimsel Granite sample; (b) typical assembly for placement of the sample into the Obert-Hoek Cell.

Test Procedure

The Grimsel Granite sample was sealed on the cylindrical surface using a neoprene rubber membrane. The ends of the sample contained porous stainless steel discs to would ensure the creation of a one dimensional flow regime in the sample. The Grimsel Granite sample was subjected to a confining stress of 5 MPa. This was achieved by alternately increasing the radial and axial stresses by increments of 0.5 MPa until the stress state corresponded to an isotropic value of 5 MPa. From the results of previous research conducted on Indiana Limestone, Stanstead Granite, Rudna Sandstone and other rocks, it was established that this value of radial stress was sufficient to prevent interface flow along the cylindrical surface of the sample provided that the pressures applied to create steady flow through the Grimsel Granite sample was less than 1 MPa.

The sample of the Grimsel Granite was subjected to fluid flow starting from its dry condition in order to establish whether the pressures at the upstream end would stabilize with time. There could be many reasons for this including creation of new fluid flow pathways as the sample became progressively saturated. Considering the limitations of attaining a steady upstream pressure for a given flow rate, the experimental procedure was changed to supplying a steady flow rate and allowing a steady pressure to develop with time. The flow rate was adjusted until the inlet pressure reached 350 kPa and upon attainment of the pressure the flow rate was reduced so that the inlet pressure stabilized at a value 250 kPa. This approach proved to be successful since low flow-rate could be achieved using a Quizix precision pump.

Results and Analysis of Data

Typical experimental results for the stabilization for the flow rate are shown in Figures 6 to 10. The permeability was calculated using the elementary relationship for one dimensional flow through a cylindrical sample of cross sectional area A and length H, maintained at an inlet pressure of p_i and an outlet pressure p_e: i.e.

$$K = \frac{Q\mu H}{A(p_i - p_e)}$$

The values of permeability estimated using the above expression and the experimental data are summarized in **Table 1**.

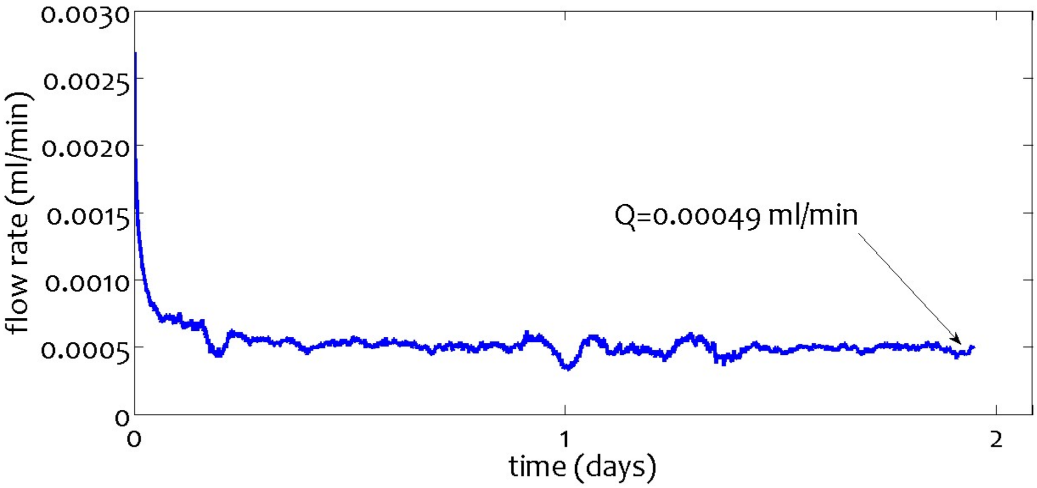

Figure 6: The results of a permeability test performed on Grimsel Granite at a constant pressure of 250 kPa at the upstream end and a constant pressure of 40 kPa at the downstream end (Test 1).

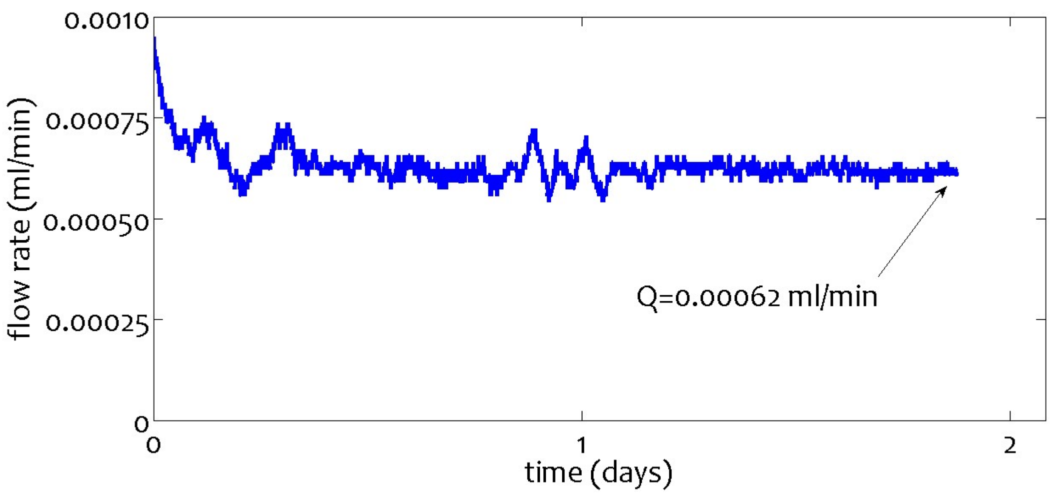

Figure 7: The results of a permeability test performed on Grimsel Granite at a constant pressure of 300 kPa at the upstream end and a constant pressure of 40 kPa at the downstream end (Test 2).

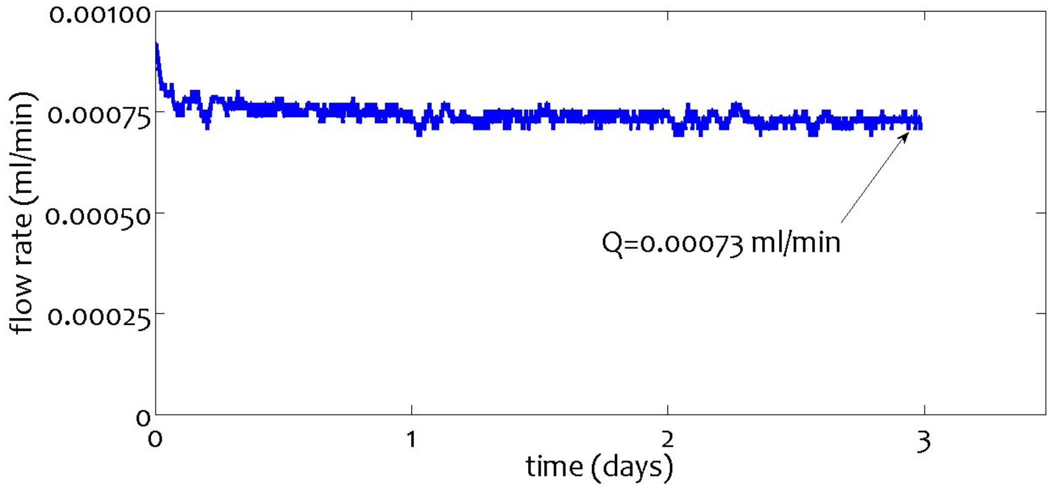

Figure 8: The results of a permeability test performed on Grimsel Granite at a constant pressure of 350 kPa at the upstream end and a constant pressure of 40 kPa at the downstream end (Test 3).

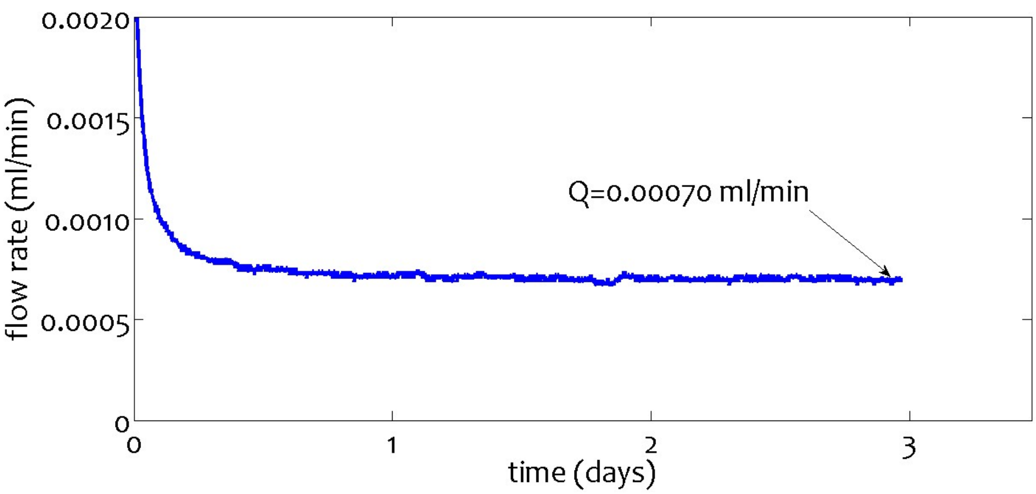

Figure 9: The results of a permeability test performed on Grimsel Granite at a constant pressure of 350 kPa at the upstream end and a constant pressure of 40 kPa at the downstream end(Test 4).

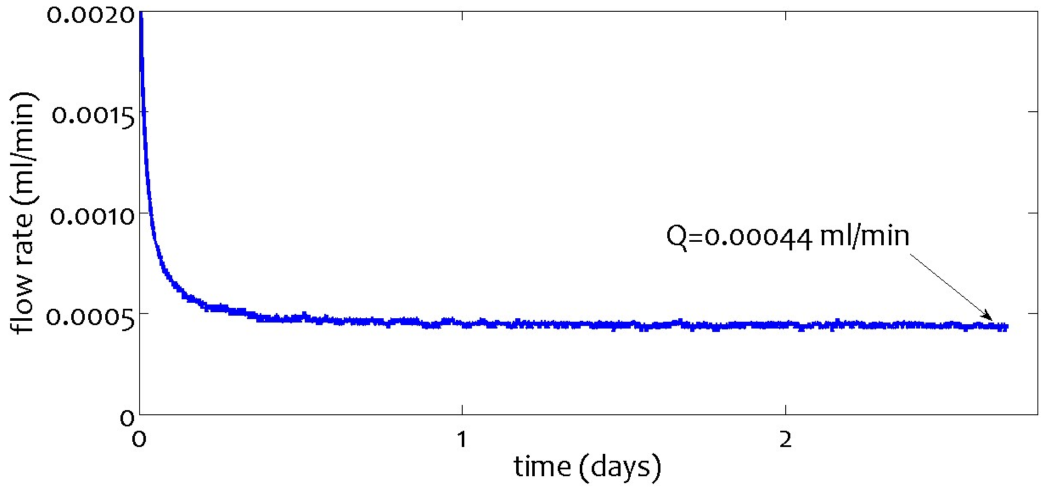

Figure 10: The results of a permeability test performed at a constant pressure of 250 kPa at the upstream end and a constant pressure of 40 kPa at the downstream end (Test 5).

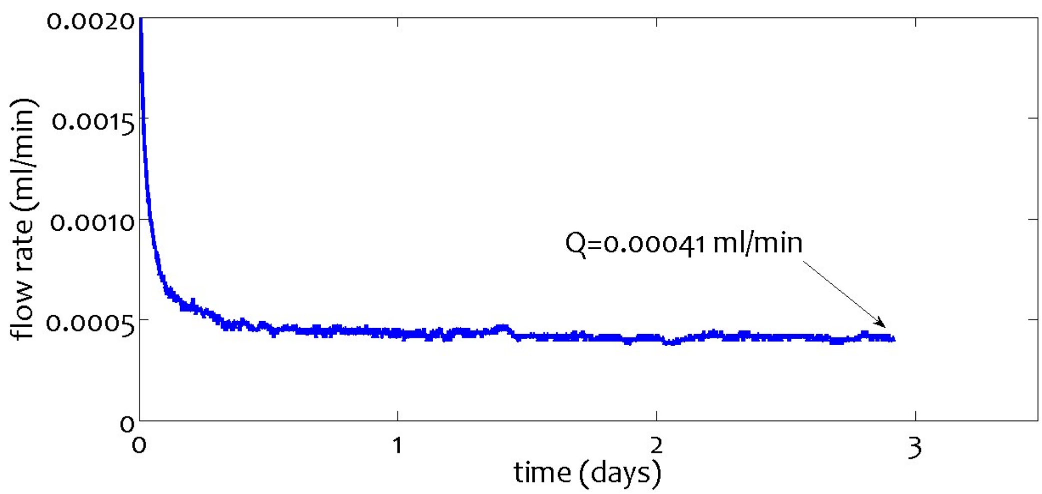

Figure 11 The results of a permeability test performed at a constant pressure of 250 kPa at the upstream end and a constant pressure of 40 kPa at the downstream end (Test 6).

Table 1: The results of permeability tests performed on the Grimsel cylindrical sample assuming that the tests were performed at 23.0 °C ambient temperature.

Test No.	$(p_i - p_e)$ (kPa)	Q (ml/min)	K (m^2)
test 1	250	0.00049	6.26×10^{-19}
test 2	300	0.00062	6.40×10^{-19}
test 3	350	0.00073	6.32×10^{-19}
test 4	350	0.00070	6.06×10^{-19}
Test 5	250	0.00044	5.62×10^{-19}
Test 6	250	0.00041	5.26×10^{-19}

Concluding Remarks

The post-permeability testing mass of the wet Grimsel Granite sample was 1398.59 g compared to the air dry mass of 1392.52 g. This corresponds to a porosity of 0.6 %. From the results of the steady state experiments completed at the Environmental Geomechanics Laboratory at McGill University, it is estimated that the permeability of the tested sample of Grimsel Granite can vary between $5.26 \times 10^{-19}\ \mathrm{m}^2$ and $6.40 \times 10^{-19}\ \mathrm{m}^2$. In general, it can be concluded that for permeabilities in the above range, steady state test conditions can be achieved in a relatively short time, as can be seen from the stable pressure gradients at relatively low flow rates. Precision pumps are therefore necessary to perform the permeability tests. The steady state test eliminates the need to estimate additional parameters such as compressibility of the porous skeleton, compressibility of the pore fluid, the Biot coefficient for the porous skeletal structure and the possibility of an air voids fraction in the pressurized fluid region that are required when conducting hydraulic pulse tests on the test specimen. It is, however, useful to perform one-dimensional hydraulic pulse tests to confirm the peremeability estimates derived from the steady state tests. Further alternate confirmatory results are in preparation.

Acknowledgements

The author would like to thank Post Doctoral Fellow Dr. Meysam Najari, doctoral student Mr. Adrian Głowacki and Chief Technician Mr. John Bartczak for their assistance in the completion of the tests.

References

Aldea C.-M., Shah S.P., Karr A. (1999) Permeability of cracked concrete, *Materials and Structures/ Matériaux et Constructions*, **32**: 370-376.

David C., Wong T.-F., Zhu W., Zhang J. (1994) Laboratory Measurement of Compaction-Induced Permeability Change in Porous Rocks: Implications for the Generation and Maintenance of Pore Pressure Excess in the Crust, *Pure and Applied Geophysics* **143**, 425-456.

Davy C., Skoczylas F., Barnichon J.-D., Lebon P. (2007) Permeability of macro-cracked argillite under confinement: gas and water testing, *Physics and Chemistry of the Earth* **32,** 667-680.

Mehta P.K., Monteiro P.J.M. (2014) *Concrete. Microstructure, Properties and Materials*, McGraw-Hill, New York.

Nabawy, B.S., David, C. (2016) X-Ray CT scanning imaging for the Nubia sandstone as a tool for characterizing its capillary properties, *Geosciences Journal*, **20**, 691-704.

Selvadurai A.P.S., Carnaffan P. (1997) A transient pressure pulse technique for the measurement of permeability of a cement grout, *Canadian Journal of Civil Engineering* **24**, 489-502.

Selvadurai A.P.S., Głowacki A. (2008) Evolution of permeability hysteresis of Indiana Limestone during isotropic compression, *Ground Water* 46, 113-119.

Selvadurai A.P.S., Głowacki A. (2017) Stress-induced permeability alterations in an argillaceous limestone, *Rock Mechanics and Rock Engineering*, DOI 10.1007/s00603-016-1153-3

Selvadurai A.P.S., Jenner L. (2012) Radial flow permeability testing of an argillaceous limestone, *Ground Water*, **51**, 1, 100-107.

Selvadurai A.P.S., Najari M. (2013) On the interpretation of hydraulic pulse tests on rock specimens, *Advances in Water Resources* **53**, 139-149.

Selvadurai A.P.S., Najari M. (2015) Laboratory-scale hydraulic pulse testing: Influence of air fraction in cavity on the estimation of permeability, *Géotechnique* **65**, 2, 126-134.

Selvadurai A.P.S., Selvadurai P.A. (2010) Surface permeability tests: Experiments and modelling for estimating effective permeability, *Proceedings of the Royal Society, Mathematical and Physical Sciences Series A* **466** (2122), 2819-2846.

Selvadurai A.P.S., Boulon M.J., Nguyen T.S. (2005) The permeability of an intact granite, *Pure and Applied Geophysics* **162**, 373-407.

Selvadurai A.P.S., Letendre A., Hekimi B. (2011) Axial flow hydraulic pulse testing of an argillaceous limestone, *Environmental Earth Sciences* **64**, 8, 2047-2058.

Vilks P., Miller N.H. (2007) *Evaluation of Experimental Protocols for Characterizing Diffusion in Sedimentary Rocks*, Atomic Energy of Canada Limited. Nuclear Waste Management Division Report TR-2007-11. Toronto, Ontario.